An Analysis on the Cutting Force Coefficient in Al_2O_3/MoS_2 Hybrid Nanofluid MQCL Hard Milling of Hardox 500 Steel

Long Tran The
Department of Manufacturing Engineering, Faculty of Mechanical Engineering, Thai Nguyen University of Technology, Thai Nguyen, Vietnam
tranthelong@tnut.edu.vn (corresponding author)

Received: 7 September 2025 | Revised: 10 November 2025, 25 November 2025, and 30 November 2025 | Accepted: 11 December 2025

 DOI: https://doi.org/10.48084/etasr.14586

ABSTRACT

Hardox 500 is a wear-resistant steel with a nominal hardness of 500 HBW and is widely recognized for its high strength, superior abrasion and impact resistance, and good toughness. These properties make it suitable for demanding applications such as heavy machinery and construction equipment. However, the elevated cutting temperatures, high cutting forces, and accelerated tool wear associated with this material present significant challenges when using conventional machining methods. Consequently, the development of sustainable cooling and lubricating techniques has become increasingly important. This study evaluates the effects of an Al_2O_3/MoS_2 hybrid nanofluid under a Minimum Quantity Cooling Lubrication (MQCL) environment on the cutting force coefficient during the hard milling of Hardox 500 steel. A Box–Behnken experimental design was employed to investigate the influence of Nanoparticle Concentration (NC), cutting speed (v), and feed rate (f) on the cutting force coefficient F_x/F_z. The results demonstrated a notable improvement in the hard milling performance of Hardox 500, with NC identified as the most influential parameter affecting F_x/F_z. Optimal ranges for the tested variables were determined as NC = 1%–1.5%, v = 80m/min –85 m/min, and f = 0.09 mm/month–0.15 mm/tooth, which collectively contributed to a reduction in F_x/F_z. The optimal combination, NC = 1.5%, v = 80 m/min, and f = 0.13 mm/tooth, yielded the lowest cutting force coefficient, F_x/F_z = 0.2269. These results were validated by confirmation experiments. The Al_2O_3/MoS_2 hybrid nanofluid MQCL condition delivered superior performance in both F_y/F_z and surface roughness (Ra) compared to dry machining, flood coolant, pure MQCL, and single-nanofluid MQCL (Al_2O_3 or MoS_2). Relative to dry, flood, and pure MQCL conditions, F_y/F_z decreased by approximately 34%, 28.8%, and 27.5%, respectively, while Ra was reduced by 37.8%, 24.6%, and 20.2%. These findings confirm that the Al_2O_3/MoS_2 hybrid nanofluid provides enhanced cooling and lubricating capability compared to individual nanofluids. Furthermore, integrating vortex-tube MQCL with the Al_2O_3/MoS_2 hybrid nanofluid for machining Hardox 500 is a key advancement and the principal contribution of this study.

Keywords-Hardox 500; hard milling; hard machining; MQL; MQCL; nanofluid; hybrid nano cutting oil; cutting force coefficient

I. INTRODUCTION

The use of hardened alloy steels with high abrasion and impact resistance has increased significantly across numerous industrial sectors [1], resulting in a growing demand for machining these materials. However, the substantial heat generation and high cutting forces involved remain major challenges, often leading to deterioration in surface quality and reduced tool life [2]. Cutting fluids are commonly employed to mitigate these issues by lowering the elevated temperatures and friction within the cutting zone. Despite their effectiveness, conventional cutting fluids pose drawbacks due to the presence of chemical components that can be harmful to both the human health and the environment [3]. In addition, the costs associated with the supply, storage, and especially the disposal of cutting oils continue to rise, creating further pressure to minimize their use or transition toward more sustainable and environmentally friendly alternatives such as vegetable oils and vegetable-based lubricants [4].

New research and application directions in industrial production have emphasized sustainable and environmentally friendly machining solutions. The hard machining technology, which refers to the processing of materials with hardness levels typically above 45 HRC, such as hardened steels, tool steels, heat-treated alloys, and superalloys, has become widely adopted as an alternative or complementary approach to traditional grinding operations [5]. Hard machining includes turning, milling, drilling, and boring of extremely hard materials using advanced cutting tools such as coated carbide, CBN, PCBN, and ceramic tools. Hard milling has been

extensively used in the mold and die industry because it enables manufacturers to achieve fine surface finishes, tight tolerances, and complex geometries directly on hardened components, often eliminating the need for secondary finishing processes [6]. However, the intense cutting heat produced during dry hard milling accelerates tool wear, causes premature tool failure, and compromises surface quality.

Additionally, when flood cooling is applied, the intermittent nature of the cutting process can cause thermal shock to the tool, further reducing its lifespan [7]. To address these challenges, the development and adoption of advanced cooling and lubrication strategies have become essential. Cryogenic cooling, Minimum Quantity Lubrication (MQL), Cryogenic MQL, and nano-enhanced MQL have all demonstrated effectiveness and have been increasingly utilized in hard machining applications. Authors in [8] optimized the cutting parameters for flat-surface milling of SKD 11 tool steel under MQL conditions, reporting that milling performance improved due to the high lubricity provided by the MQL technique. The use of vegetable oil as the base fluid in MQL ensures effective lubrication while maintaining environmentally friendly characteristics. However, the cooling capability of conventional MQL remains limited, prompting the development of advanced methods such as MQL and nano-enhanced MQL. Authors in [9] examined the machinability of Ti-6Al-4V during milling under cryogenic cooling and nanofluid MQL conditions. Their results demonstrated that combining nanofluid MQL with cryogenic cooling provided superior outcomes in terms of tool wear, surface residual stress, and cutting temperature, compared with using cryogenic cooling or nanofluid MQL alone. Similarly, authors in [10] reported significant improvements across various milling operations when using MQL mixed with nanofluids, primarily due to enhanced cooling and lubrication performance relative to dry and flood cooling modes. The integration of nanoparticles into the base oil also enables secondary lubrication mechanisms [11]. Authors in [12] found that higher concentrations of an Al_2O_3/graphene hybrid nanofluid contributed to smoother surfaces during the hard turning of AISI D3 tool steel by reducing friction, lowering wear, improving heat conductivity, forming a protective layer, and increasing viscosity. In [13], it was reported that the combination of statistical optimization, machine learning, and Al_2O_3/graphene hybrid nanofluid cooling significantly enhanced surface quality, thermal efficiency, and Material Removal Rate (MRR) when machining AISI D2 tool steel. Furthermore, authors in [14] demonstrated the high lubricating effectiveness of MoS_2- and graphite-reinforced nanofluid MQL during the turning of Inconel 625. Compared with dry machining and conventional MQL, the nanofluid MQL conditions reduced cutting temperatures, slowed tool wear progression, and improved surface quality. The concentrations of MoS_2 and graphite nanoparticles were identified as highly influential factors.

Vegetable-oil-based graphene nanofluids with varying mass fractions were used in [15] for the MQL milling of 7075 aluminum alloy. The study showed that a 0.5 wt% graphene nanofluid achieved the highest thermal conductivity and lower viscosity relative to pure vegetable oil, resulting in reduced friction, lower cutting temperatures, and decreased cutting forces. Authors in [16] concluded that water-graphene nanofluids represent an eco-friendly alternative to traditional metalworking fluids, offering improved sustainability in machining operations. Additionally, authors in [17] identified a strong relationship between Al_2O_3 NC and base-oil characteristics; Al_2O_3 additions in coconut oil improved wettability, dynamic viscosity, and thermal conductivity. The "rolling" or "micro-bearing" effect of Al_2O_3 nanoparticles also reduced tool wear and enhanced surface quality [18]. MQCL represents an advanced stage of MQL technology intended to improve cooling performance. In [19], MQCL was compared with dry machining during the end milling of Inconel 718, with MQCL (using biodegradable vegetable oil) producing significantly better results in terms of cutting forces and tool life. Higher machining performance of Ti-6Al-4V under MQCL compared with wet machining was, likewise, reported in [20]. Despite these advancements, limited research is available regarding the application of MQCL systems based on the Ranque–Hilsch vortex tube principle combined with nanofluid cutting oils [21]. Therefore, the present study focuses on this approach to enhance the hard-milling performance of Hardox 500 steel, a material known for its high strength, toughness, and machinability challenges. The extreme cutting temperatures and accelerated tool wear are typically encountered when machining Hardox 500 necessitate a highly efficient cooling and lubrication method. The introduction of an Al_2O_3/MoS_2 hybrid nanofluid into an MQCL system is a promising solution; however, existing research on this topic remains scarce.

In this study, an MQCL device (Frigid-X Sub-Zero Vortex Tool Cooling Mist System, Nex Flow™, Richmond Hill, Canada) was used in combination with an Al_2O_3/MoS_2 hybrid nanofluid during the hard milling of Hardox 500 steel. The effects of key process parameters, NC, cutting speed, and feed rate, on the cutting force ratio F_x/F_zwere analyzed to identify suitable operational ranges and optimal conditions for practical applications. Authors in [22] examined the total cutting force f and the force ratio F_y/F_z, defined as the ratio of axial (passive) force to tangential (primary) force. This ratio reflects the relative contribution of elastic deformation forces and is particularly useful for evaluating flank wear and tool machinability in hard-material cutting. The present study focuses on the relationship between the feed force F_x and tangential force F_z, both classified as active force components. For difficult-to-cut materials, like Hardox 500 steel, analyzing this ratio is critical for understanding the cutting performance and assessing tool machinability.

II. MATERIALS AND METHODS

The setup for the hard milling experiments has been described in [22]. A single cutting edge was used for each experimental run and replaced with a new edge after every test to ensure measurement consistency. Al_2O_3 and MoS_2 nanoparticles (30 nm) were dispersed in soybean oil at a weight ratio of 8:2 (wt%), following the recommendations from [12, 18]. The preparation procedure for the Al_2O_3/MoS_2 hybrid nanofluid is illustrated in Figure 1. The mixture was mechanically stirred and then subjected to ultrasonic agitation using a SELECTA Ultrasons-HD (Spain) device for 1 h to

ensure proper homogenization of nanoparticles within the vegetable oil. The resulting hybrid nanofluid was used directly in the MQCL system. During machining, the MQCL nozzle was directed toward the flank face of the cutting tool at a spray angle of 15° [10]. The system parameters consisted of an air pressure of 6 bar and an oil flow rate of 30 ml/h [10, 24]. Cutting force components were measured using a Kistler quartz three-component dynamometer (Type 9257BA), connected to a DQA N16210 A/D data acquisition unit (National Instruments, USA), operating at a sampling interval of 0.001 s. The definitions of the force components follow those presented in [22]: F_z is the tangential cutting force responsible for material removal, while Fx is the feed force (f), acting in the direction of tool advancement. Hardox 500 steel specimens with dimensions of 150 mm × 100 mm × 15 mm were used in all experiments. The chemical composition and mechanical properties of Hardox 500 steel are summarized in Tables I and II.

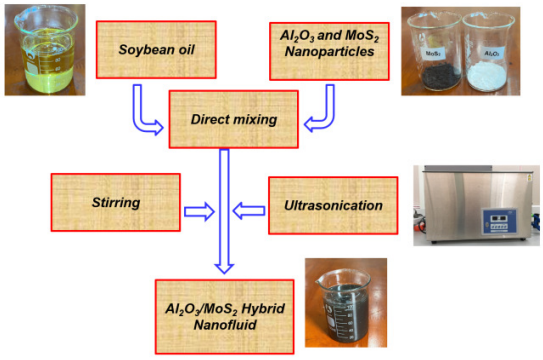

Fig. 1. Preparation process of Al_2O_3/MoS_2 hybrid nanofluid.

TABLE I. ELEMENTAL COMPOSITION OF HARDOX 500 STEEL

Element	Composition (%)
C	0.3
Si	0.7
Mn	1.6
P	0.25
S	0.01
Cr	1.5
Ni	1.5
Mo	0.6
B	0.005

TABLE II. MECHANICAL PROPERTIES OF HARDOX 500 STEEL

Yield strength, MPa	Tensile strength, MPa	Elongation, %	Hardness range, HBW	Hardness range, HRC
1250	1400	10	470 - 530	49 - 50

The Box-Behnken response surface methodology was employed to design the experiments, as it requires fewer runs and avoids extreme conditions at the corners of the experimental space [13, 24]. This approach is more efficient and safer, particularly when extreme runs are risky or costly, and the number of factors is low (three) [25, 26]. The investigated variables and their levels are listed in Table III, based on [12, 22]. Hard milling trials were conducted according to the experimental matrix, with each run repeated three times under the same cutting conditions. The average cutting force values were then calculated and recorded in Table IV.

TABLE III. INPUT VARIABLES AND RESPONSES

Input variables	Low level	High level	Output variable
NC (wt%)	0.5	1.5	Cutting force coefficient F_x/F_z
Cutting speed, v (m/min)	80	140	
Feed rate, f (mm/tooth)	0.08	0.16	

III. RESULTS AND DISCUSSION

Minitab 19 software was used to analyze the experimental data at a significance level of $\alpha = 0.05$. The fit between the experimental data and the proposed model was assessed using the coefficient of determination, $R^2 = 71.44\%$. The regression equation for the cutting force coefficient F_x/F_z is:

$$\frac{F_x}{F_z} = -0.94 + 1.077\,NC + 0.02233\,v - 6.27f - 0.393\,NC \times NC - 0.000096\,v \times v + 28.7\,f \times f - 0.00177\,NC \times v - 1.77\,NC \times f + 0.0146\,v \times f \quad (1)$$

Based on the results of the Analysis of Variance (ANOVA) analysis for the cutting force coefficient F_x/F_z (Table V), the Square model has the highest percentage contribution of 42.14%. In the meantime, the Linear model ranks second with a rate of 23.95%, and the least influence is that of the 2-Way Interaction with a rate of 5.35%. Considering the effect of each surveyed factor on the models, in the Linear model, NC has highest percentage contribution of 67.14% with a P-value smaller than 0.05 [13, 27], followed by the cutting speed with a value of 26.43%, while the feed rate has negligible impacts with a percentage contribution rate of 6.43%, as confirmed by a P-value of 0.312. For the Square model, the second-order interaction NC × NC has the greatest effect (49.67%), followed by v × v with a percentage contribution of 38.35%. Also, the second-order interaction f × f has an insignificant effect (11.98%). The two-way interactions of the investigated variables have a negligible influence on the cutting force coefficient F_x/F_z, with P-values greater than 0.05 [28].

For the cutting force coefficient F_x/F_z shown in Figure 2, the coefficient initially increases as the NC rises from 0.5% to approximately 0.8%. However, it then decreases sharply as NC is further increased up to 1.5%. A similar trend is observed for the cutting speed. As the cutting speed (v) increases from 80 m/min to 120 m/min, the F_x/F_z coefficient increases, but it subsequently decreases when the cutting speed is raised from 120 m/min to 140 m/min.

TABLE IV. SUMMARY OF THE EXPERIMENTAL DESIGN AND THE CUTTING FORCE COEFFICIENTS F_X/F_Z

Std Order	Run Order	PtType	Blocks	Input parameters			Responses			
				NC (%)	v (m/min)	f (mm/tooth)	F_x (N)	F_y (N)	F_z (N)	F_x/F_z
1	10	2	1	0.5	80	0.12	72.5	156.8	270.9	0.268
2	2	2	1	1.5	80	0.12	70.4	210.5	310.2	0.227
3	1	2	1	0.5	140	0.12	71.3	145.2	260.8	0.273
4	18	2	1	1.5	140	0.12	67.8	164.9	250.4	0.271
5	16	2	1	0.5	110	0.08	64.8	93.5	139.6	0.464
6	22	2	1	1.5	110	0.08	85.7	140.2	200.1	0.428
7	4	2	1	0.5	110	0.16	85.5	114.7	168.4	0.508
8	24	2	1	1.5	110	0.16	95.7	230.5	318.8	0.300
9	30	2	1	1	80	0.08	67.2	110.5	178.9	0.376
10	12	2	1	1	140	0.08	60.8	105.2	174.5	0.348
11	29	2	1	1	80	0.16	128	190.3	264.8	0.483
12	27	2	1	1	140	0.16	147.5	237.9	265.6	0.555
13	15	0	1	1	110	0.12	85.2	125.2	167.8	0.508
14	6	0	1	1	110	0.12	81.4	125.9	170.8	0.477
15	11	0	1	1	110	0.12	80.5	122.7	170.4	0.472
16	14	2	1	0.5	80	0.12	70.5	154.8	274.6	0.257
17	5	2	1	1.5	80	0.12	75.2	200.9	314.8	0.239
18	28	2	1	0.5	140	0.12	89.6	103.6	155.7	0.575
19	9	2	1	1.5	140	0.12	75.4	168.9	245.9	0.307
20	13	2	1	0.5	110	0.08	73.8	97.4	136.9	0.539
21	23	2	1	1.5	110	0.08	87.3	150.2	210.7	0.414
22	3	2	1	0.5	110	0.16	61.8	89.8	116.9	0.529
23	21	2	1	1.5	110	0.16	90.5	235.9	310.4	0.292
24	19	2	1	1	80	0.08	65.8	112.8	169.9	0.387
25	8	2	1	1	140	0.08	75.6	110.6	180.1	0.420
26	7	2	1	1	80	0.16	120.6	188.7	260.5	0.463
27	25	2	1	1	140	0.16	145.1	240.8	270.5	0.536
28	20	0	1	1	110	0.12	81.3	123.9	172.6	0.471
29	26	0	1	1	110	0.12	80.5	124.2	168.9	0.477
30	17	0	1	1	110	0.12	65.8	108.9	127.9	0.514

TABLE V. ANOVA RESULTS FOR THE CUTTING FORCE COEFFICIENT F_X/F_Z

Source	DF	Adj SS	Adj MS	F-Value	P-Value	PCR%	PCR%
Model	9	0.242880	0.026987	5.56	0.001		
Linear	3	0.081416	0.027139	5.59	0.006	23.95	
NC(%)	1	0.054670	0.054670	11.26	0.003*		67.14
V(m/min)	1	0.021517	0.021517	4.43	0.048*		26.43
f (mm/tooth)	1	0.005229	0.005229	1.08	0.312		6.43
Square	3	0.143261	0.047754	9.84	0.000	42.14	
NC(%)×NC(%)	1	0.071154	0.071154	14.66	0.001*		49.67
V (m/min) ×V (m/min)	1	0.054947	0.054947	11.32	0.003*		38.35
f (mm/tooth) ×f (mm/tooth)	1	0.015582	0.015582	3.21	0.088		11.98
2-Way Interaction	3	0.018203	0.006068	1.25	0.318	5.35	
NC(%)×V(m/min)	1	0.005667	0.005667	1.17	0.293		31.13
NC(%)×f(mm/tooth)	1	0.010081	0.010081	2.08	0.165		55.38
V(m/min) ×f(mm/tooth)	1	0.002455	0.002455	0.51	0.485		13.49
Error	20	0.097080	0.004854			28.56	
Lack-of-Fit	3	0.042655	0.014218	4.44	0.018		
Pure Error	17	0.054425	0.003201				
Total	29	0.339960				100	

For f =0.08÷0.1 mm/min, the F_x/F_z value slightly falls and then grows with f =0.1÷0.16 mm/min. This shows the significant influence of the feed force. Therefore, it is meaningful to study this force component and its ratio to the tangential forces. Specifically, for increasing NC from 0.8% to 1.5%, the values of F_x/F_z decrease significantly. This reflects the phenomenon of impedance, collision, and uneven penetration into the cutting zone of the hybrid nano cutting fluid due to the increase in the number of nanoparticles [18, 23].

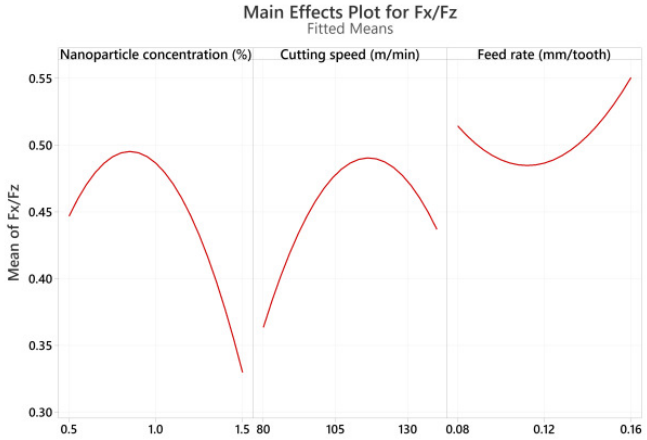

Fig. 2. Main effects of surveyed factors on F_x/F_z.

The effects of the surveyed factors on F_x/F_z are shown in Figures 3-5. In Figure 3, for f = 0.12 mm/tooth, the high level of NC used with the low cutting speed will achieve the smallest F_x/F_z (Figure 3(a)). Looking in detail, NC=1.5% and v =80 m/min are selected to achieve the cutting force coefficient F_x/F_z <0.25, which is the dark red area in Figure 3(b). In case of v = 110 m/min, f = 0.1mm/tooth to 0.15 mm/tooth, and NC = 1.4%÷1.5% are chosen to reach the smaller F_x/F_z <0.35, as shown in Figure 4. When NC is fixed at 1%, f = 0.09 mm/tooth to 0.15 mm/tooth and v =80 m/min to 85 m/min are chosen to get the smaller F_x/F_z <0.4 (Figure 5).

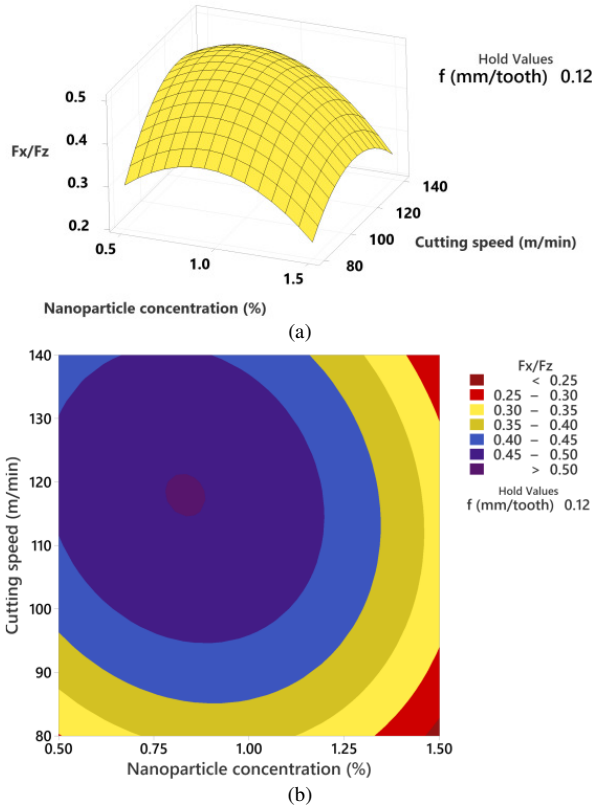

Fig. 3. (a) Surface plot and (b) contour plot of NC and cutting speed on F_x/F_z.

Thus, the following parameter ranges were selected to achieve smaller F_x/F_z values: NC = 1%–1.5%, v = 80 m/min to 85 m/min, and f = 0.09 mm/tooth to 0.15 mm/tooth. Exhaust fans and the ventilation system removed the nanoparticle-containing oil mist generated by the MQCL system to ensure operator safety and address environmental concerns.

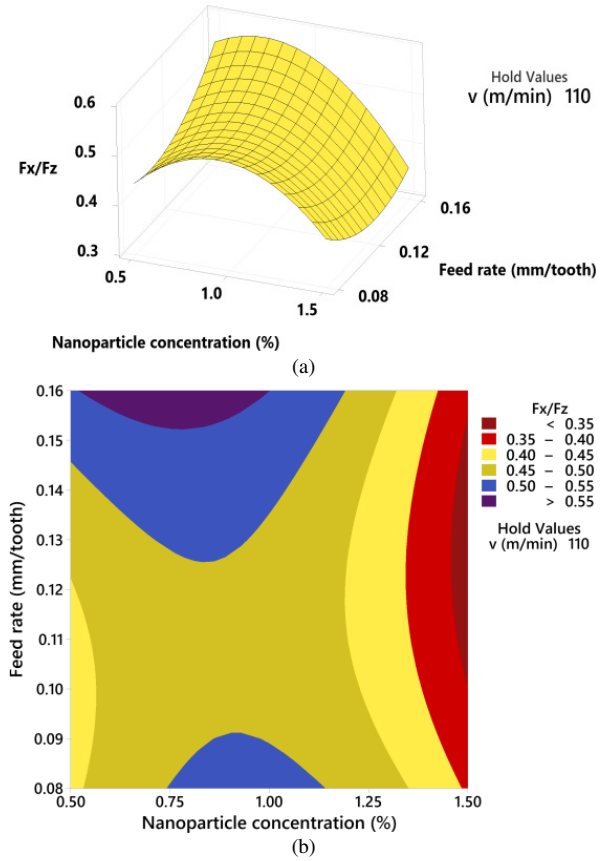

Fig. 4. (a) Surface plot and (b) contour plot of NC and feed rate on F_x/F_z.

Based on the obtained results from the surface and contour graphs, the appropriate value ranges were specified; however, the optimization process should be done to find out the exact values. The minimum value of F_x/F_z =0.2269 is achieved with the optimal set of NC=1.5%, v =80 m/min, and f=0.13 mm/tooth after rounding, as depicted in Figure 6.

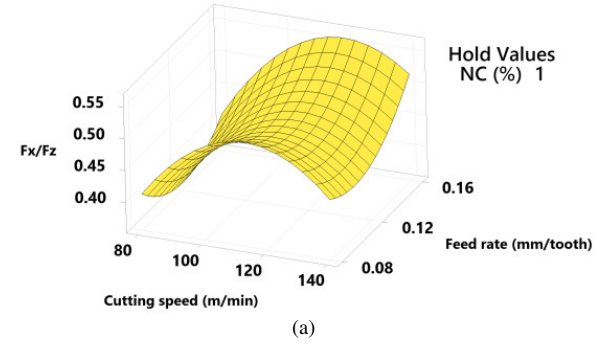

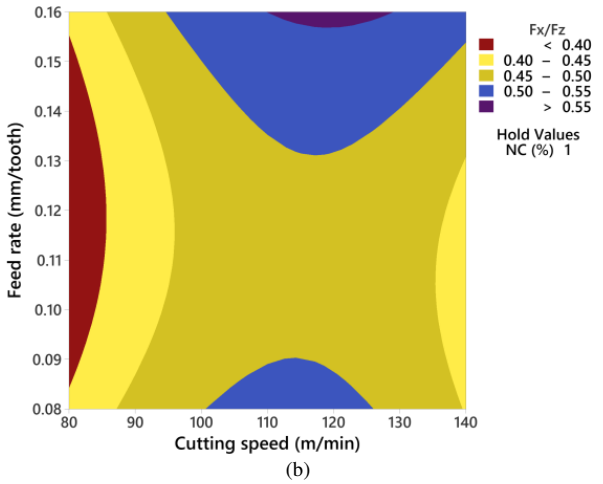

(b)

Fig. 5. (a) Surface plot and (b) contour plot of cutting speed and feed rate on F_x/F_z.

The confirmation experiments were conducted three times using the predicted optimal parameters: NC = 1.5%, v = 80 m/min, and f = 0.13 mm/tooth. The average measured cutting force components were F_x = 70.6 N, F_y = 210.7 N, and F_z = 310.8 N. This corresponds to F_x/F_z = 0.2272, resulting in a deviation of only 0.13% from the predicted value, which is considered acceptable [28]. To further evaluate the effectiveness of the Al_2O_3/MoS_2 hybrid nanofluid MQCL, additional experiments were performed under various cooling–lubrication conditions, including dry cutting, flood coolant, pure MQCL, Al_2O_3 nanofluid MQCL, and MoS_2 nanofluid MQCL. The process parameters were fixed at NC = 1.5%, v = 80 m/min, and f = 0.13 mm/tooth. The measured values of Ra and cutting force coefficient (F_x/F_z) are presented in Figure 7. Among all tested conditions, the Al_2O_3/MoS_2 hybrid nanofluid MQCL exhibited the best performance, showing significant reductions in both F_x/F_z and Ra. Compared with dry cutting, F_x/F_z and Ra decreased by 34% and 37.8%, respectively. Relative to flood coolant, the reductions were 28.8% and 24.6%, respectively. These results demonstrate the improvement in machining performance. Both nanofluid MQCL and hybrid-nanofluid MQCL outperformed pure-oil MQCL, confirming the superior cooling and lubricating capabilities provided by nanoparticles.

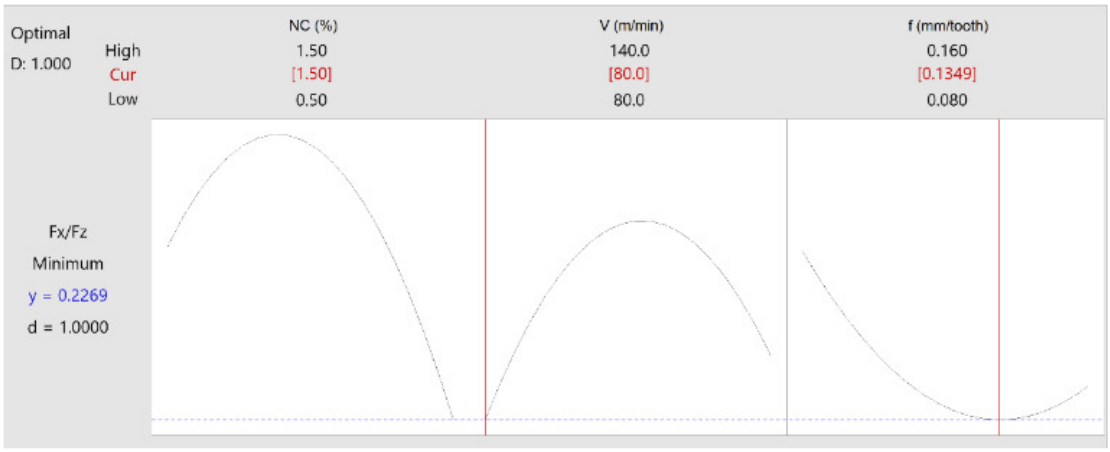

Fig. 6. Optimization result for F_x/F_z.

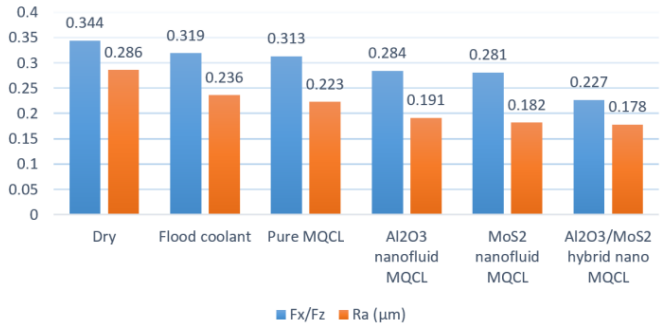

Fig. 7. R_a and F_x/F_z under different cooling lubrication modes.

The exhaust fans and ventilation system treated the oil mist containing nanoparticles generated by the MQCL system to ensure operator safety and minimize environmental impact.

IV. CONCLUSIONS

In this study, the effects of NC, cutting speed, and feed rate on the cutting force coefficient F_x/F_z were investigated for the the hard milling of Hardox 500 steel (49–50 HRC) using an Al_2O_3/MoS_2 hybrid nanofluid in an MQCL environment. The key findings are: The use of Al_2O_3/MoS_2 hybrid nanofluid in the MQCL system significantly enhanced lubrication and cooling in the tool–workpiece and tool–chip contact zones. The combined secondary lubrication mechanisms provided by Al_2O_3 nanoparticles and MoS_2 nanosheets contributed to notable improvements in MQCL efficiency and hard-milling performance. This enhancement is reflected in the allowable cutting speed range for coated carbide inserts, which increased from the manufacturer-proposed 50–55 m/min to 110–140 m/min. The results also confirm the feasibility of extending vegetable-oil-based cutting fluids to hard milling applications, supporting the sustainability of this approach. The analysis showed that NC and its quadratic term exert the strongest

influence on F_x/F_z, contributing 67.14% and 49.67%, respectively. Cutting speed and its quadratic effect represent the second most influential factors. Based on the response behavior, the proposed ranges for achieving lower F_x/F_z values are NC = 1%–1.5%, v = 80–85 m/min, and f = 0.09–0.15 mm/tooth. Single-objective optimization identified NC = 1.5%, v = 80 m/min, and f = 0.13 mm/tooth (rounded) as the optimal parameter set, yielding a minimum F_x/F_z value of 0.2269. The confirmation experiments demonstrated that the Al_2O_3/MoS_2 hybrid nanofluid MQCL condition achieved superior results in both Ra and cutting force coefficient (F_x/F_z) compared with dry cutting, flood coolant, pure MQCL, Al_2O_3 nanofluid MQCL, and MoS_2 nanofluid MQCL. Compared with dry, flood, and pure MQCL conditions, F_x/F_z decreased by approximately 34%, 28.8%, and 27.5%, respectively, while Ra decreased by 37.8%, 24.6%, and 20.2%. These outcomes confirm that the hybrid nanofluid provides more effective cooling and lubrication than single-nanoparticle formulations. For future work, further investigations should focus on the surface microstructure, tool-wear mechanisms, and overall machining efficiency under MQCL using Al_2O_3/MoS_2 hybrid nanobiodegradable oils.

ACKNOWLEDGMENT

The study was supported by Thai Nguyen University of Technology, Thai Nguyen University, Vietnam.

REFERENCES

[1] V. P. Astakhov, "Machining of Hard Materials – Definitions and Industrial Applications," in *Machining of Hard Materials*, J. P. Davim, Ed. London: Springer, 2011, pp. 1–32.

[2] K. Nakayama, M. Arai, and T. Kanda, "Machining Characteristics of Hard Materials," *CIRP Annals*, vol. 37, no. 1, pp. 89–92, Jan. 1988, https://doi.org/10.1016/S0007-8506(07)61592-3.

[3] H. Çalışkan, C. Kurbanoğlu, P. Panjan, M. Čekada, and D. Kramar, "Wear behavior and cutting performance of nanostructured hard coatings on cemented carbide cutting tools in hard milling," *Tribology International*, vol. 62, pp. 215–222, June 2013, https://doi.org/10.1016/j.triboint.2013.02.035.

[4] T. Nguyen, V. T. Nguyen, V. C. Nguyen, T. D. Hoang, N. H. Dao, and H. D. Minh, "The Prediction and Optimization of Surface Roughness in Grinding of S50c Carbon Steel Using Minimum Quantity Lubrication of Vietnamese Peanut Oil," *Journal of Applied Engineering Science*, vol. 19, no. 3, pp. 813–820, May 2021, https://doi.org/10.5937/jaes0-30580.

[5] Y. Huo, Y. Niu, Z. Sun, Y. Li, and J. Niu, "Surface/subsurface damage mechanisms and inhibition strategies in machining of hard and brittle materials: A systematic review," *Surfaces and Interfaces*, vol. 54, Nov. 2024, Art. no. 105088, https://doi.org/10.1016/j.surfin.2024.105088.

[6] K. Bouacha, M. A. Yallese, T. Mabrouki, and J.-F. Rigal, "Statistical analysis of surface roughness and cutting forces using response surface methodology in hard turning of AISI 52100 bearing steel with CBN tool," *International Journal of Refractory Metals and Hard Materials*, vol. 28, no. 3, pp. 349–361, May 2010, https://doi.org/10.1016/j.ijrmhm.2009.11.011.

[7] Y. Su, Z. Li, L. Li, J. Wang, H. Gao, and G. Wang, "Cutting performance of micro-textured polycrystalline diamond tool in dry cutting," *Journal of Manufacturing Processes*, vol. 27, pp. 1–7, June 2017, https://doi.org/10.1016/j.jmapro.2017.03.013.

[8] V. H. Pham, T. D. Nguyen, V. T. Le, D. H. Tien, and V.-C. Nguyen, "Optimization of Cutting Parameters in MQL Flat Surface Milling of SKD11 Steel," in *Proceedings of the International Conference on Advanced Mechanical Engineering, Automation, and Sustainable Development 2021 (AMAS2021)*, Cham, 2022, pp. 261–266, https://doi.org/10.1007/978-3-030-99666-6_40.

[9] S. H. Ju, T.-G. Kim, S.-W. Lee, H.-J. Choi, and J. Nam, "Machinability of Ti-6Al-4 V in the milling process using cryogenic cooling and nanofluid MQL," *Journal of Manufacturing Processes*, vol. 152, pp. 568–578, Oct. 2025, https://doi.org/10.1016/j.jmapro.2025.08.030.

[10] A. P. Vadnere and S. D. Kalpande, "A review on effects of process parameters in milling challenging materials under nanofluid-based MQL conditions," *Industrial Lubrication and Tribology*, vol. 75, no. 4, pp. 361–371, Mar. 2023, https://doi.org/10.1108/ILT-01-2023-0010.

[11] N. A. C. Sidik, S. Samion, J. Ghaderian, and M. N. A. W. M. Yazid, "Recent progress on the application of nanofluids in minimum quantity lubrication machining: A review," *International Journal of Heat and Mass Transfer*, vol. 108, pp. 79–89, May 2017, https://doi.org/10.1016/j.ijheatmasstransfer.2016.11.105.

[12] L. D. Gemechu, D. A. Efa, and R. Abebe, "Optimizing CNC turning of AISI D3 tool steel using Al_2O_3/graphene nanofluid and machine learning algorithms," *Heliyon*, vol. 10, no. 24, Dec. 2024, https://doi.org/10.1016/j.heliyon.2024.e40969.

[13] D. A. Efa, N. D. Dejene, D. A. Ifa, S. K. Nemomsa, and T. B. Gemechu, "Improving computer numerical control (CNC) turning performance of AISI D2 steel with nanofluid composites and advanced machine learning techniques," *The International Journal of Advanced Manufacturing Technology*, vol. 138, no. 2, pp. 511–539, May 2025, https://doi.org/10.1007/s00170-025-15536-5.

[14] M. A. Makhesana, K. M. Patel, G. M. Krolczyk, M. Danish, A. K. Singla, and N. Khanna, "Influence of MoS2 and graphite-reinforced nanofluid-MQL on surface roughness, tool wear, cutting temperature and microhardness in machining of Inconel 625," *CIRP Journal of Manufacturing Science and Technology*, vol. 41, pp. 225–238, Apr. 2023, https://doi.org/10.1016/j.cirpj.2022.12.015.

[15] R. Peng, J. Shen, X. Tang, L. Zhao, and J. Gao, "Performances of a tailored vegetable oil-based graphene nanofluid in the MQL internal cooling milling," *Journal of Manufacturing Processes*, vol. 134, pp. 814–831, Jan. 2025, https://doi.org/10.1016/j.jmapro.2024.12.063.

[16] A. M. M. Ibrahim, W. Li, Z. Zeng, B. H. Bedairi, and A. ElSheikh, "Graphene nanoplatelets-water nanofluids: A sustainable approach to enhancing Ti-6Al-4V grinding performance through minimum quantity lubrication," *Tribology International*, vol. 201, Jan. 2025, Art. no. 110145, https://doi.org/10.1016/j.triboint.2024.110145.

[17] S. Tiwari, M. Amarnath, and M. K. Gupta, "Synthesis, characterization, and application of Al2O3/coconut oil-based nanofluids in sustainable machining of AISI 1040 steel," *Journal of Molecular Liquids*, vol. 386, Sept. 2023, Art. no. 122465, https://doi.org/10.1016/j.molliq.2023.122465.

[18] F. Günan, T. Kıvak, Ç. V. Yıldırım, and M. Sarıkaya, "Performance evaluation of MQL with AL2O3 mixed nanofluids prepared at different concentrations in milling of Hastelloy C276 alloy," *Journal of Materials Research and Technology*, vol. 9, no. 5, pp. 10386–10400, Sept. 2020, https://doi.org/10.1016/j.jmrt.2020.07.018.

[19] S. Zhang, J. F. Li, and Y. W. Wang, "Tool life and cutting forces in end milling Inconel 718 under dry and minimum quantity cooling lubrication cutting conditions," *Journal of Cleaner Production*, vol. 32, pp. 81–87, Sept. 2012, https://doi.org/10.1016/j.jclepro.2012.03.014.

[20] N. Anand, A. S. Kumar, and S. Paul, "Effect of cutting fluids applied in MQCL mode on machinability of Ti-6Al-4V," *Journal of Manufacturing Processes*, vol. 43, pp. 154–163, July 2019, https://doi.org/10.1016/j.jmapro.2019.05.029.

[21] P. Q. Dong, T. M. Duc, and T. T. Long, "Performance Evaluation of MQCL Hard Milling of SKD 11 Tool Steel Using MoS2 Nanofluid," *Metals*, vol. 9, no. 6, June 2019, Art. no. 658, https://doi.org/10.3390/met9060658.

[22] T. T. Long, "Experimental Investigation on Cutting Forces in Sustainable Hard Milling of Hardox 500 Steel Under Al2O3/MoS2 Hybrid Nanofluid MQCL Environment," *Lubricants*, vol. 13, no. 6, June 2025, Art. no. 240, https://doi.org/10.3390/lubricants13060240.

[23] B. Rahmati, A. A. D. Sarhan, and M. Sayuti, "Morphology of surface generated by end milling AL6061-T6 using molybdenum disulfide (MoS2) nanolubrication in end milling machining," *Journal of Cleaner Production*, vol. 66, pp. 685–691, Mar. 2014, https://doi.org/10.1016/j.jclepro.2013.10.048.

[24] D. A. Efa, E. M. Gutema, H. G. Lemu, and M. Gopal, "Friction stir-welding of AZ31B Mg and 6061-T6 Al alloys optimization using Box-Behnken design (BBD) and Artificial Neural Network (ANN)," *Research on Engineering Structures & Materials*, vol. 10, no. 1, pp. 413–430, Oct. 2023, [Online]. Available: https://jresm.org/article/resm2023-50ma0703rs/.

[25] D. A. Efa and D. A. Ifa, "Optimization of design parameters and 3D-printing orientation to enhance the efficiency of topology-optimized components in additive manufacturing," *Results in Materials*, vol. 26, June 2025, Art. no. 100702, https://doi.org/10.1016/j.rinma.2025.100702.

[26] D. A. Ifa, D. A. Efa, N. D. Dejene, and S. K. Nemomsa, "Physics-informed modeling and process optimization of friction stir welding of AA7075-T6 with a zinc interlayer," *Next Materials*, vol. 9, Oct. 2025, Art. no. 100999, https://doi.org/10.1016/j.nxmate.2025.100999.

[27] T. V. Do and N. A. V. Le, "Development of a Multi-Objective Optimization Model for the Hard Turning of SKD11 Steel with Nanofluid-Al_2O_3 Minimum Quantity Lubrication Using RSM and PSO," *Engineering, Technology & Applied Science Research*, vol. 15, no. 4, pp. 24897–24903, Aug. 2025, https://doi.org/10.48084/etasr.11351.

[28] V. C. Nguyen, N. N. Ba, D. H. Tien, Q. N. Van, X. T. Nguyen, and T. N. Thuy, "Using Support Vector Regression and Non-Dominated Sorting Genetic Algorithm in Multi-Objective Optimization of Milling of S50c Steel Under MQL Condition," *Journal of Applied Engineering Science*, vol. 20, no. 1, pp. 123–130, Jan. 2022, https://doi.org/10.5937/jaes0-31366.

AUTHORS PROFILE

Dr. Tran The Long is a lecturer and researcher of the Department of Manufacturing Engineering, Mechanical Engineering Faculty at Thai Nguyen University of Technology, Thai Nguyen University, Vietnam. He received his Ph.D degree from Thai Nguyen University of Technology in 2023. His research focused on the machining of difficult-to-cut materials, MQL, MQCL, nanofluid, nano cutting oil, green manufacturing, and sustainable machining.